J. Gen. Appl. Microbiol., **62**, 118–125 (2016)
doi 10.2323/jgam.2015.12.002

jGAM

Full Paper

Isolation and characterization of a bacterial strain that degrades *cis*-dichloroethene in the absence of aromatic inducers

(Received August 10, 2015; Accepted December 25, 2015; J-STAGE Advance publication date: May 23, 2016)

Kenta Yonezuka,[1] Naoto Araki,[1] Jun Shimodaira,[2] Shoko Ohji,[2] Akira Hosoyama,[2] Mitsuru Numata,[2] Atsushi Yamazoe,[2] Daisuke Kasai,[1] Eiji Masai,[1] Nobuyuki Fujita,[2] Takayuki Ezaki[3], and Masao Fukuda[1,*]

[1] *Department of Bioengineering, Nagaoka University of Technology, 1603-1 Kamitomioka, Nagaoka, Niigata 940-2188, Japan*
[2] *Biological Resource Center, National Institute of Technology and Evaluation, 2-49-10 Nishihara, Shibuya-ku, Tokyo 151-0066, Japan*
[3] *Department of Microbiology, Gifu University Graduate School of Medicine, 1-1 Yanagido, Gifu 501-1194, Japan*

Bacteria capable of degrading *cis*-dichloroethene (cDCE) were screened from cDCE-contaminated soil, and YKD221, a bacterial strain that exhibited a higher growth on minimal salt agar plates in the presence of cDCE than in the absence of cDCE, were isolated. Phylogenetic studies of the 16S rRNA as well as *gyrB*, *rpoD*, and *recA* in YKD221 indicated that this strain is closely related to the type strains of *Pseudomonas plecoglossicida*, *monteilii*, and *putida*. An average nucleotide identity analysis indicated that YKD221 is most closely related to *P. putida* strains, including the type strain, which suggests that YKD221 belongs to *P. putida*. Although the genome of YKD221 was very similar to that of *P. putida* F1, a toluene-degrading strain, the YKD221 genome has 15 single-nucleotide polymorphisms and 4 insertions compared with the F1 genome. YKD221 caused the release of sufficient chloride ions from cDCE to suggest that the strain is able to completely dechlorinate and degrade cDCE. YKD221 also degraded trichloroethene but was unable to degrade *trans*-dichloroethene and tetrachloroethene. The degradation activity of YKD221 was elevated after growth on toluene. Inactivation of *todC1*, which encodes for a large subunit of the catalytic terminal component in toluene dioxygenase, resulted in a complete loss of growth on toluene and cDCE degradation activity. This is the first evidence of the involvement of *todC1C2BA*-coded toluene dioxygenase in cDCE degradation. YKD221 did not appear to grow on cDCE in a minimal salt liquid medium. However, YKD221 did exhibit an enhanced increase in cell concentration and volume of cells during growth on minimal salt agar plates with cDCE when first grown in LB medium. This behavior appears to have led us to misinterpret our initial results on YKD221 as an indication of improved growth in the presence of cDCE.

Key Words: *cis*-dichloroethene; *Pseudomonas*; toluene dioxygenase; trichloroethene

Introduction

Tetrachloroethene (PCE) and trichloroethene (TCE) have been widely used as organic solvents in many industries, including the metal processing, semiconductor, and dry cleaning industries. However, unexpected leakages of these solvents into the soil and groundwater from factories have caused problematic environmental contamination throughout the world (ATSDR 2011 substance priority list). Microbial biodegradation is a promising solution to environmental chloroethene contamination. PCE and TCE can be degraded to ethene by reductive dehalogenases found in anaerobic bacteria including those in the genus *Dehalococcoides* (Fig. 1) (Futagami et al., 2008; Maymo-Gatell et al., 1999). However, incomplete degradation, which sometimes occurs, is known to result in the accumulation of hazardous intermediate substances such as *cis*-

*Corresponding author: Masao Fukuda, Department of Bioengineering, Nagaoka University of Technology, 1603-1 Kamitomioka, Nagaoka, Niigata 940-2188, Japan.
Tel: +81-258-47-9405 Fax: +81-258-47-9450 E-mail: masao@vos.nagaokaut.ac.jp

None of the authors of this manuscript has any financial or personal relationship with other people or organizations that could inappropriately influence their work.

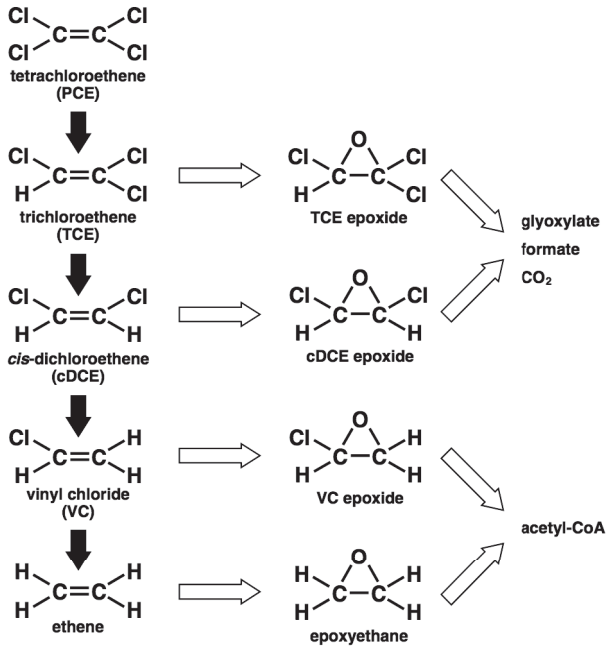

Fig. 1. Deduced degradation pathway of chlorinated ethenes.

Pathway is illustrated based on the literature cited (Arp et al., 2001; Coleman and Spain, 2003; Futagami et al., 2008; Jennings et al., 2009; Li and Wackett, 1992; Magnuson et al., 1998; Mattes et al., 2005, 2010; Newman et al., 1997). Anaerobic and aerobic degradation steps are represented by filled and open arrows, respectively.

dichloroethene (cDCE) and vinyl chloride (VC) (Futagami et al., 2008; Maymo-Gatell et al., 1999).

The ability to degrade TCE has been reported in many aerobic bacteria, including the toluene-degrading strains *Pseudomonas putida* F1 (Wackett and Gibson, 1988), *Pseudomonas mendocina* KR1 (McClay et al., 1995), and *Ralstonia pickettii* PKO1 (Leahy et al., 1996), the phenol-degrading strain *Burkholderia cepacia* G4 (Nelson et al., 1987), the methane-degrading strains *Methylosinus trichosporium* OB3b (Tsien et al., 1989) and *Methylosicystis* sp. M (Uchiyama et al., 1992), and the ammonium-degrading strain *Nitrosomonas europaea* (Arciero et al., 1989). These bacteria employ dioxygenases or monooxygenases to degrade not only their target substrates (toluene, phenol, methane, or ammonium) but also TCE. These oxygenases are believed to convert TCE to TCE epoxide, which is further transformed to glyoxylate or formate as illustrated in Fig. 1. Because these oxygenases are induced in the presence of their target substrate, the target substrate must be present for the co-metabolic degradation of TCE. An exception is the phenol-degrading strain *Wautersia numazuensis* TE26, which has been shown to degrade TCE in the absence of an inducing substrate (Kageyama et al., 2005).

Co-metabolic degradation of cDCE has been observed in toluene-degrading strains, such as F1, KR1, and PKO1, and is believed to proceed via a route similar to that illustrated in Fig. 1 (Clingenpeel et al., 2012; Wackett and Gibson, 1988). Similar degradation routes have also been hypothesized for VC and ethene degradation by alkene monooxygenases in the ethene-assimilating bacteria *Mycobacterium* sp. JS60 and *Nocardioides* sp. JS614 (Fig. 1) (Coleman and Spain, 2003; Mattes et al., 2005).

The same oxygenases are believed to be responsible for both TCE and cDCE degradation via epoxides. *Polaromonas* sp. JS666, a cDCE-degrading strain, has been reported to grow marginally on cDCE (Coleman et al., 2002). Strains JS666 and TE26 degraded cDCE without any inducing substrates (Coleman et al., 2002; Kageyama et al., 2005). These bacteria appear to be useful for removing cDCE, which accumulates during anaerobic degradation, from the environment.

In order to develop a strain that can be used for bioremediation without inducing substrates, cDCE-degrading aerobic bacteria were selected from cDCE-contaminated soils in this study. An isolate that exhibited strong degradation activity in the absence of inducing substrates was then characterized.

Materials and Methods

Bacterial strains, plasmids, culture conditions, and chemicals. The bacterial strains and plasmids used in this study are listed in Table 1. YKD221 and *E. coli* strains were grown at 30°C and 37°C, respectively. Strains were grown in the following media: W medium composed of 1.7 g of KH_2PO_4, 9.8 g of Na_2HPO_4, 1.0 g of $(NH_4)_2SO_4$, 0.1 g of $MgSO_4{\cdot}7H_2O$, 9.5 mg of $FeSO_4{\cdot}7H_2O$, 10.75 mg of MgO, 2.0 mg of $CaCO_3$, 1.44 mg of $ZnSO_4{\cdot}7H_2O$, 1.12 mg of $MnSO_4{\cdot}4H_2O$, 0.25 mg of $CuSO_4{\cdot}5H_2O$, 0.28 mg of $CoSO_4{\cdot}7H_2O$, 0.06 mg of H_3BO_3, and 51.3 μl of 12 N HCl per liter; LB medium composed of 10 g of Bacto Tryptone, 5 g of yeast extract, and 5 g of NaCl per liter; 1/5 LB medium composed of 2 g of Bacto Tryptone, 1 g of yeast extract, and 5 g of NaCl per liter; or R2A agar composed of 0.5 g of yeast extract, 0.5 g of Proteose Peptone No. 3, 0.5 g of Casamino Acids, 0.5 g of Dextrose, 0.5 g of Soluble Starch, 0.3 g of sodium pyruvate, 0.03 g of dipotassium phosphate, and 0.05 g of magnesium sulfate per liter. If necessary, 15 g of agar, 25 mg of kanamycin, 25 mg of nalidixic acid, or 100 g of sucrose per liter were added to the medium. cDCE, *trans*-dichloroethene (tDCE), TCE, PCE, and toluene were supplied in vapor as sole carbon sources.

Isolation of cDCE-degrading bacteria. Soil samples were collected from Akita, Chiba, Niigata, and Osaka, in Japan. Ten grams of soil were placed in a 120-ml glass vial and 100 μl of W medium, 100 μl of cDCE, 100 μl of a solution containing 167 mM urea and 15 mM KH_2PO_4, and 50 mg of activated carbon powder were added to grow microorganisms individually in the solid-phase-like conditions. Sample vials were sealed with Teflon-coated butyl rubber stoppers and aluminum caps, then incubated at 30°C with rotary shaking at 15 rpm. Each vial was opened every 15 days to add the amounts of W medium, cDCE, urea, and KH_2PO_4 described above and to remove 0.5 g of soil. Vials were then resealed, and incubation was continued for a total of six months. A 0.2-g aliquot of the 0.5-g of soil removed from each vial was suspended in 5 ml of W containing 0.5% (w/v) agar and overlaid on a W medium agar plate. Plates were incubated for approximately 7 days at 30°C with cDCE in a sealed container. Any colonies that appeared on the plates were transferred in duplicate

Table 1. Strains and plasmids used in this study.

Strain or Plasmid	Relevant characteristic(s)	Reference or source
Bacterial strains		
Pseudomonas sp. YKD221	A wild-type cDCE degrader, Nal^r, Tol$^+$	This study
Pseudomonas sp. YKD221ΔtodC1	A derivative of YKD221 with the 1,323-bp *todC1* deletion, Nal^r, Tol$^-$	This study
Escherichia coli S17-1	*recA*, *pro*, *hsdR*, RP4-2-TC::Mu in the chromosome	Simon et al. (1983)
Escherichia coli JM109	*recA*1, *supE44*, *endA1*, *hsdR17*, *gyrA96*, *relA1*, *thi*, Δ(*lac-proAB*) F′ [*traD36 proAB*$^+$ *lacI*^{q} *lacZ*ΔM15]	Yanisch-Perron et al. (1985)
Plasmids		
pK18mobsacB	pMB1 *ori*, *oriT* (RP4), *sacB*, Kan^r	Schäfer et al. (1994)
pK18ΔtodC1	pK18mobsacB carrying the Δ*todC1* construct	This study

Tol$^+$, growth on toluene, Tol$^-$, no growth on toluene, Kan^r, resistance to kanamycin, Nal^r, resistance to nalidixic acid.

to fresh W agar plates and incubated at 30°C with, or without, cDCE in a sealed container. Colonies that exhibited better growth in the presence of cDCE than in the absence of cDCE were subjected to single colony isolation using LB, 1/5 LB, or R2A agar plates. Among the 12 candidate strains that we obtained, we chose YKD221 to investigate further, because this strain showed a superior cDCE degradation activity compared with the other strains.

Degradation activity assay. Cells were grown to mid-log phase in LB liquid medium, or overnight on LB agar plates. Toluene-induced cells were grown for 24 hours on W agar plates with toluene supplied as a vapor, then collected by suspending in 5 ml of W liquid medium followed by centrifugation. These cells were washed three times with W liquid medium then suspended in W liquid medium to an OD_{600} of 10. One ml of cell suspension was added to a 20-ml glass vial containing 500 μM of chlorinated ethenes, sealed with a Teflon-coated butyl rubber stopper and an aluminum cap, and incubated at 30°C with shaking at 180 rpm. Autoclaved dead cells were used as a control to avoid interference from chlorinated ethene leakage out of sealed vials as well as adsorption of chlorinated ethenes to cell surfaces and the butyl rubber stopper. Depletion of chlorinated ethenes was measured by quantifying the amount of chlorinated ethenes remaining in the headspace of a sealed vial. Headspace gas of 250 μl was subjected to gas chromatography with flame ionization detection (GC-FID) using an Agilent 7890A GC (Agilent, Palo Alto, CA, USA) equipped with a GC sampler 80 (Agilent) and a DB-624 capillary column (30 m by 0.32 mm, J&W Scientific, Folsom, CA, USA). The oven temperature was held for 5 min at 35°C, then increased to 165°C at 30°C/min, and held constant at 165°C for 1 min (total runtime: 10.3 min). The injection and detection temperatures were 200°C and 250°C, respectively. Chlorinated ethene peaks were detected at the following retention times: cDCE, 5.01 min; tDCE, 3.34 min; TCE, 6.82 min; PCE, 8.10 min. Peak areas were auto-integrated by the Agilent ChemStation software (Agilent) to determine the amount of chlorinated ethene remaining in each vial.

To determine the amount of chloride ion released, precultured cells were washed three times with 10 mM phosphate buffer (pH 7.0) and resuspended to an OD_{600} of 10 in 10 mM phosphate buffer (pH 7.0) instead of W liquid medium, which contains a large amount of chloride ions. A sealed vial containing 1 ml of cell suspension and 500 μM of chlorinated ethenes was incubated at 30°C with shaking at 180 rpm. Heat-killed cells were used as a control to avoid interference from chloride ions released by the cells. Depletion of chlorinated ethenes was determined as described above; release of chloride ion was quantified by ion chromatography (IC) using an Ion Analyzer IA-300 instrument (DKK-TOA, Tokyo, Japan). After GC-FID analysis, the cell suspension was centrifuged, and the supernatant was filtered through a 0.22 μm syringe filter. A 100 μl aliquot was diluted with 900 μl of filtered MilliQ water and subjected to IC analysis according to the manufacturer's instructions. IC calibration was performed using a NaCl solution of known concentration.

Determination of the number and size of cells during growth on cDCE. YKD221 cells grown in LB liquid medium were washed three times with W liquid medium and resuspended in W liquid medium to a concentration of approximately 5.0×10^7 cells/ml. One ml of cell suspension was placed in a 100-ml glass vial containing 500 μM of cDCE to keep enough oxygen for an oxygenase reaction, sealed with a Teflon-coated butyl rubber stopper and an aluminum cap, and incubated at 30°C without shaking. Every three days, a 100-μl aliquot of the culture was transferred to a 100-ml glass vial containing 900 μl of fresh W liquid medium with, or without, 500 μM of cDCE and incubated at 30°C without shaking. An aliquot of cell suspension was diluted and spread onto LB agar plates, and the concentration of living cells was determined by colony counting after incubation. The sizes of YKD221 cells after incubation with, or without, 500 μM of cDCE were determined by microscopic observation after Gram staining. Gram staining of cells was performed according to the standard procedure (Murray et al., 1994).

Sequence analysis. The 16S rRNA gene of YKD221 was amplified by PCR using the universal primer pair (10F and 1500R, Table S1) and sequenced using the ABI 3730 DNA Analyzer (Applied Biosystems, Foster City, CA, USA). The draft genome of YKD221 was sequenced using a combined strategy of shotgun sequencing with 454 GS FLX Titanium (Roche Diagnostics, Branford, CT, USA) and paired-end sequencing with MiSeq 1000 (Illumina, Inc., San Diego, CA, USA). The obtained data were assembled using Newbler version 2.6. The assembled draft sequence of the YKD221 genome was analyzed using the Microbial Genome Annotation Pipeline (MiGAP, http://www.migap.org/), which predicts protein-coding,

tRNA, and rRNA genes. Functional annotations of the predicted protein-coding genes were assigned based on UniProt, InterPro, HAMAP, and an in-house database composed of manually curated microbial genome sequences, as reported previously (Shintani et al., 2013).

Nucleotide sequences of the housekeeping genes *gyrB*, *rpoD*, and *recA*, as well as genes involved in toluene degradation, were extracted from the draft genome sequence of YKD221. The draft genome sequence was then aligned with reference sequences obtained from the National Center for Biotechnology Information (NCBI) and the Biological Resource Center of the National Institute of Technology and Evaluation (NBRC) databases using the ClustalW algorithm within MEGA (version 5.0, http://www.megasoftware.net/index.php, Tamura et al., 2011). Phylogenetic trees based on the 16S rRNA and *gyrB* gene sequences of YKD221 and related type strains were drawn using the neighbor-joining and maximum-likelihood methods (Saitou and Nei, 1987). The 16S rRNA, *gyrB*, *rpoD*, *recA*, and the toluene-degradation genes were analyzed against the NCBI BLASTN database (http://blast.ncbi.nlm.nih.gov/Blast.cgi). The average nucleotide identity (ANI) was calculated using JSpecies with the default settings for ANI based on BLAST (http://www.imedea.uib.es/jspecies). Single nucleotide polymorphisms (SNPs) between YKD221 and *P. putida* F1 were identified by mapping YKD221 raw read sequences to F1 complete genome sequence (Accession No. CP000712) using GS Reference Mapper version 2.8 (Roche Diagnostics). The draft genome sequence of YKD221 was deposited in the GenBank nucleotide sequence database under the accession number of BBNC01000001–BBNC01000091.

Construction of a gene deletion mutant. DNA manipulations were performed essentially as described by Ausubel et al. (1990) and Sambrook et al. (1989). The region containing the upstream terminal 15-bp sequences of and the connecting upstream 1,045-bp sequences from *todC1* were amplified from YKD221 genomic DNA by PCR using the primer pair, FtodC1_FP and FtodC1_RP (Table S1). The region containing the downstream terminal 15-bp sequences of and the connecting downstream 988-bp sequences from *todC1* were amplified using the primer pair, RtodC1_FP and RtodC1_RP. A vector plasmid, pK18mobsacB, was linearized by EcoRI digestion and ligated with the upstream and downstream PCR products using an In-Fusion HD Cloning kit (Takara Bio, Otsu, Japan) according to the manufacturer's protocols. The structure of the resulting recombinant plasmid, pK18ΔtodC1, was confirmed by restriction enzyme analysis. pK18ΔtodC1 was introduced into YKD221 by conjugal transfer using *E. coli* S17-1, and kanamycin-resistant transconjugants were selected in the presence of kanamycin and nalidixic acid. The *todC1*-deletion mutant with sucrose resistance, which results from allelic exchange, was selected in the presence of sucrose as described previously (van der Geize et al., 2001). The deletion of *todC1* in the resulting mutant was confirmed by colony PCR using the primers todC1C2_F and todC1C2_R (Table S1) as well as the inability to grow on toluene. This mutant was designated YKD221ΔtodC1.

Results and Discussion

Isolation and identification of the selected strain

Screening of cDCE-degrading bacteria was performed by selecting the candidates able to grow on minimal salt medium plates in the presence of cDCE, to obtain bacteria able to degrade cDCE in the absence of inducing substances. The isolate YKD221 formed a larger colony in the presence of cDCE than in its absence, suggesting that YKD221 grows better in the presence of cDCE than in the absence of cDCE. YKD221 exhibited good cDCE degradation activity as described in the next section. To determine the taxonomic position of YKD221, the 16S-rRNA gene sequence of YKD221 was amplified by PCR, sequenced, and compared with 16S-rRNA sequences from *Pseudomonas* type strains to generate the phylogenetic tree depicted in Fig. 2A using the neighbor-joining method. The phylogenetic tree created using the maximum-likelihood method was essentially the same as Fig. 2A. These results indicated that the 16S-rRNA gene sequence of YKD221 is most similar to *Pseudomonas plecoglossicida* type strain NBRC 103162 with a 99.8% identity (Table S2). However, YKD221 also showed a high identity with the type strains *P. monteilii* NBRC 103158 and *P. putida* NBRC 14164 (99.6% and 99.1%, respectively). To verify the taxonomic position of YKD221, draft genome sequencing of YKD221 was performed, and the sequence of *gyrB*, a DNA gyrase, was used to generate another phylogenetic tree of YKD221 and *Pseudomonas* type strains (Fig. 2B). The *gyrB* phylogenetic tree suggests that YKD221 is more related to *P. monteilii* and *P. putida* than *P. plecoglossicida*. Comparison of the *rpoD* and *recA* sequences encoding RNA polymerase sigma factor and recombinase A suggests the same notion (Table S2). Then, ANI analysis of YKD221 and *Pseudomonas* type strains was performed to determine definitively the taxonomic position of YKD221 (Fig. 2C). We included the *P. putida* strains F1 and KT2440 in the ANI analysis because F1 is a well-known degrader of toluene and TCE and KT2440 is a versatile host strain derived from the famous toluene-degrading *P. putida* strain mt-2. The phylogenetic tree generated by ANI analysis indicated that the strains F1, KT2440, and YKD221 are closely related and that they are slightly more related to *P. putida* NBRC 14164 than to *P. monteilii* NBRC 103158. However, the ANI percentage values between YKD221 and *P. putida* NBRC 14164 and between YKD221 and *P. monteilii* NBRC 103158 are less than 90%. These results suggest that YKD221 belongs to neither *P. putida* nor *P. monteilii*, as an ANI percentage value of 95% has been proposed to be the border between species (Auch et al., 2010; Goris et al., 2007). ANI percentages between YKD221 and F1 and between YKD221 and KT2440 are approximately 100% and 97%, respectively, suggesting that YKD221, F1, and KT2440 form a new species. These results also reveal that genome sequences are very similar between F1 and YKD221. Between them 15 SNPs were found, four of which are located in coding regions. The YKD221 genome has four insertions of 81-, 100-, 113-, and 191-bp compared with the F1 genome. Because these SNPs and insertions are not located around aromatic or alkane degradation genes,

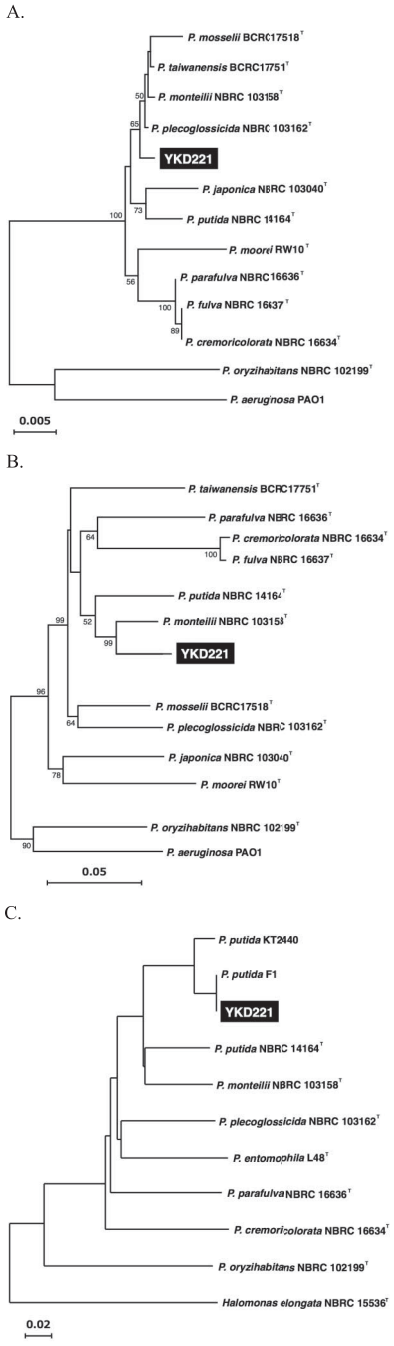

Fig. 2. Phylogenetic trees based on the 16S-rRNA gene sequences (A), the *gyrB* gene sequences (B), and the ANI analysis (C) of the strain YKD221 and the *Pseudomonas* type strains.

The scale bars in the panels A and B stand for substitutions per nucleotide position. Numbers at the nodes indicate levels of bootstrap support (%) based on a neighbor-joining analysis of 1,000 re-sampled datasets; only values above 50% are given. The scale bar in the panel C represents the ANI value. The accession numbers of the 16S rRNA and *gyrB* gene sequences are: *P. moorei* RW10^T, NR_042542 and AM293560; *P. mosselii* BCRC17518^T, AF072688 and FJ418640; *P. taiwanensis* BCRC17751^T, FJ418634 and EU103629, respectively. The nucleotide sequences of the other strains used were obtained from their genome sequences. The accession numbers of the genome sequences are: *P. plecoglossicida* NBRC103162^T, BBIV01000001–BBIV01000097; *P. monteilii* NBRC103158^T, BBIS01000001–BBIS01000132; *P. putida* NBRC14164^T, AP013070; *P. putida* KT2440, AE015451; *P. putida* F1, CP000712; *P. fulva* NBRC16637^T, BBIQ01000001–BBIQ01000046; *P. parafulva* NBRC16636^T, BBIU01000001–BBIU01000055; *P. japonica* NBRC103040^T, BBIR01000001–BBIR01000162; *P. cremoricolorata* NBRC16634^T, BBIP01000001–BBIP01000041; *P. oryzihabitans* NBRC102199^T, BBIT01000001–BBIT01000034; *P. entomophila* L48^T, CT573326; *P. aeruginosa* PAO1, AE004091; *Halomonas elongata* NBRC15536^T, FN869568.

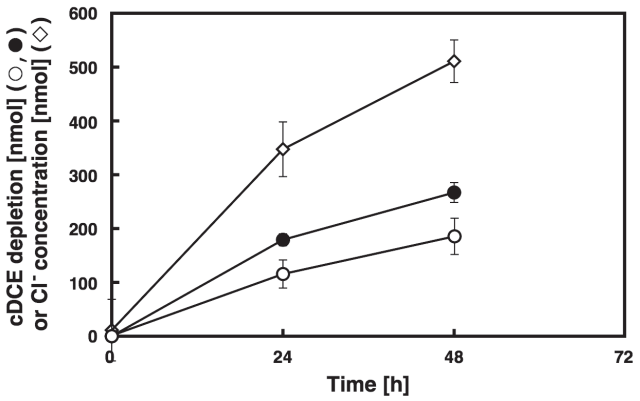

Fig. 3. Depletion of cDCE and release of chloride ions from cDCE by YKD221.

Cells suspended in 1 ml of 10 mM phosphate buffer (pH 7.0) at OD_{600} of 10.0 were encapsulated with 500 nmol cDCE in a sealed vial and the amount of cDCE depletion was estimated by headspace GC-FID. The release of chloride ions in the cell suspension was estimated by IC. The net depletion of cDCE by living cells, which was estimated by subtracting the background cDCE depletion with autoclaved cells, is represented by open circles. The overall depletion of cDCE by living cells is represented by filled circles. The net release of chloride ions from cDCE, which was estimated by subtracting indigenous chloride ions observed with autoclaved cells, is indicated by open diamonds. Each value is the average ± standard deviation (error bars) based on three independent experiments.

it is difficult to deduce the sequence difference that is responsible for the difference in chloroethene degradation activity between them. It is noteworthy that strains isolated from Japan and the United States share very similar genome sequences.

Degradation activity of YKD221 on chloroethenes

Resting YKD221 cells, which were grown in LB medium and suspended in 1 ml minimal salt medium, depleted nearly 500 nmol of cDCE within 48 hours (data not shown). These results indicated good YKD221 degradation activity on cDCE. Autoclaved dead cells of YKD221 appeared to deplete a small amount of cDCE, suggesting that a small fraction of cDCE adsorbs to dead YKD221 cells. The release of chloride ions during cDCE depletion was examined in 1 ml phosphate buffer to estimate the proportion of released chloride ion to the amount of cDCE depleted (Fig. 3). The degradation activity of YKD221 decreased approximately 50% in phosphate buffer, resulting in the depletion of 267 nmol of cDCE in 48 hours. Because 82 nmol of cDCE adsorbed to autoclaved cells, cDCE degradation by living YKD221 cells was estimated to be 185 nmol. Over 48 hours, 722 nmol of chloride ions was released by living YKD221 cells, while 211 nmol of chloride ions was released from the autoclaved cells (data not shown). These data suggest that 511 nmol of chloride ions released was associated with cDCE degradation (Fig. 3). A cDCE molecule has two chlorine atoms, so the amount of chlorine atoms released from cDCE should be twice the amount of cDCE that is depleted. This estimation does not agree with our results, however. Probably cDCE molecules adsorbed to dead cells were degraded in the living cells and it is deduced that a total of 267 nmol

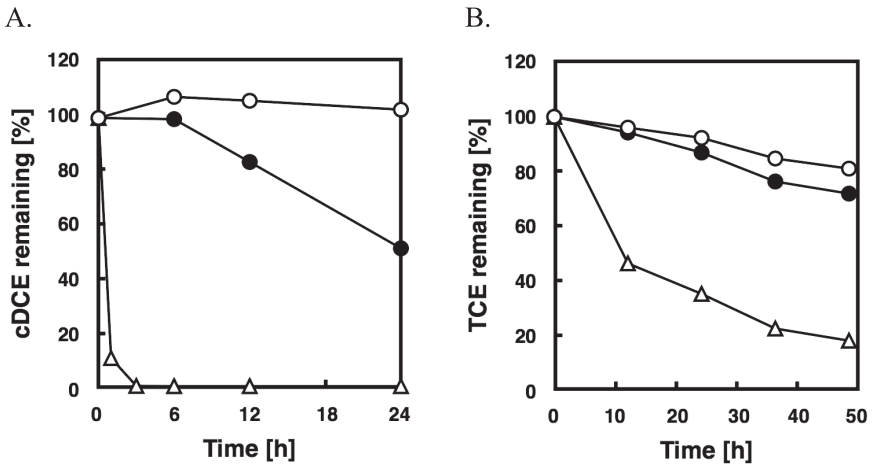

Fig. 4. Degradation activities on cDCE (A) and TCE (B) of YKD221 grown in the presence of toluene.

Cells grown on toluene on a W minimal salt agar plate or grown on a LB agar plate were washed and resuspended in 1 ml of W minimal salt medium at OD_{600} of 10.0 and degradation activities on 500 nmol of cDCE or TCE were determined by headspace GC-FID. Autoclaved cells were used as a control. The results with cells grown on toluene, cells grown on a LB agar plate, and autoclaved cells are specified by open triangles, filled circles, and open circles, respectively.

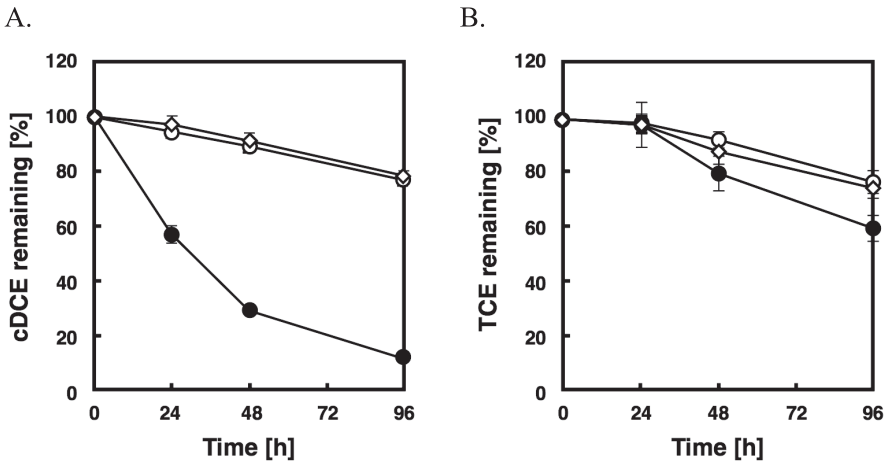

Fig. 5. Effect of *todC1* gene inactivation in YKD221 on the degradation of cDCE (A) and TCE (B).

Cells grown in LB medium were washed and resuspended in 1 ml of W minimal salt medium at OD_{600} of 10.0 and degradation activities on 500 nmol of cDCE or TCE were determined by headspace GC-FID. Autoclaved cells were used as a control. The results obtained with YKD221, autoclaved, and *todC1*-inactivated cells are indicated by filled circles, open circles, and open diamonds, respectively. Each value is the average ± standard deviation (error bars) based on three independent experiments.

of cDCE was degraded to form 511 nmol of chloride ions by living YKD221 in 48 hours. In this case, the amount of released chloride ions (511 nmol) is 1.91-fold greater than the amount of cDCE depleted (267 nmol). Regardless, the amount of chloride ions released specifically from living cells was about twice as much as the amount of cDCE depleted by the living cells, indicating that YKD221 efficiently degrades cDCE and removes most of the chlorine atoms from cDCE.

To determine the range of substrates that YKD221 can degrade, the degradation activity of YKD221 on tDCE, TCE, and PCE was examined. YKD221 resting cells in 1 ml minimal salt medium degraded approximately 150 nmol out of 500 nmol TCE within four days, but the cells were unable to degrade tDCE and PCE (data not shown). Additionally, the degradation activity of YKD221 on cDCE was far greater than that on TCE.

Toluene-dependent cDCE degradation activity of YKD221

It was reported that the toluene-inducible toluene dioxygenase encoded by *todC1C2BA* is responsible for TCE degradation in *P. putida* F1 (Wackett and Gibson, 1988). Because the genome sequence of YKD221 is very similar to the sequence of F1, toluene-inducible toluene dioxygenase may be involved in TCE degradation in YKD221. To examine this hypothesis, the growth of YKD221 on toluene and the degradation of TCE by YKD221 after growth on toluene were investigated. YKD221 grew well on toluene (data not shown) and ex-

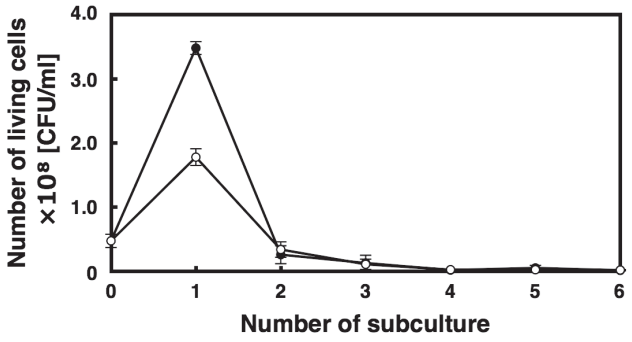

Fig. 6. Transient increase of the cell concentration during successive culture transfers in the presence of cDCE.

Cells grown in LB medium were washed, inoculated into 1 ml of W minimal salt medium at the final concentration of 4.8×10^7 cells/ml, and incubated at 30°C without shaking. Successive culture transfers were performed every three days by inoculating 0.1 ml of the culture into 0.9 ml of W minimal salt medium. Each culture was incubated at 30°C without shaking in the presence (filled circles) or absence (open circles) of 500 μM of cDCE. The cell concentration of each culture was determined by the colony counting method after spreading the appropriate dilution of the culture on LB agar plates and incubating plates overnight at 30°C. Each value is the average ± standard deviation (error bars) based on three independent experiments.

hibited a strong degradation activity on TCE after growth on toluene (Fig. 4). When YKD221 was grown in LB medium, the cells showed a weak degradation activity on TCE. These results suggest that YKD221 has a toluene-inducible TCE degradation activity similar to F1. We then searched for a toluene degradation gene cluster in the genome sequence of YKD221 and found a gene cluster with exactly the same nucleotide sequence as the *tod* gene cluster in F1.

To examine the involvement of *todC1C2BA*-coded toluene dioxygenase in TCE and cDCE degradation, *todC1*, which encodes a large subunit of the catalytic terminal component of the toluene dioxygenase, was knocked out. The pK18ΔtodC1 plasmid containing adjacent upstream and downstream sequences from *todC1* was introduced into YKD221. YKD221ΔtodC1, in which most of *todC1* is deleted, was obtained by allelic exchange between the wild-type *todC1* in the YKD221 genome and the *todC1*-deleted sequence of pK18ΔtodC1 following a double crossover event. The deletion mutant did not grow on toluene (data not shown) and showed no degradation activity on cDCE (Fig. 5A). YKD221ΔtodC1 also exhibited little degradation activity on TCE (Fig. 5B). These results indicate that degradation activity on both TCE and cDCE is dependent on the *todC1C2BA*-coded toluene dioxygenase in YKD221. This study reports the first evidence of the involvement of *todC1C2BA*-coded toluene dioxygenase in cDCE degradation.

Growth of YKD221 in the presence of cDCE

Because YKD221 was screened based on superior growth on minimal salt agar plates in the presence of cDCE, we expected that YKD221 assimilated cDCE as a sole carbon source. However, the growth of YKD221 on minimal salt agar plates in the presence of cDCE was so poor that it was difficult to detect apparent colonies. We therefore examined YKD221 growth in liquid minimal salt medium in the presence or absence of cDCE. YKD221 cells grown in LB medium were washed with, and inoculated in, minimal salt medium. Growth in minimal salt medium was repeated six times and the cell concentration of each culture was determined by spreading the cell suspension on LB agar plates after appropriate dilutions. In the first round of growth, the cell concentrations in the presence and absence of cDCE unexpectedly increased by 7.3 and 3.8 fold, respectively, compared with that at the start, 4.8×10^7 CFU/ml (Fig. 6). In the next five rounds of growth, however, cultures grown in the absence and presence of cDCE reached similar concentrations, which are significantly lower than those of the first round of growth. Cell concentrations in the following two rounds of growth decreased to around 1×10^7 CFU/ml and those in the last three rounds of growth converged to around 2×10^6 CFU/ml independently with the presence of cDCE. The cDCE independent cell concentrations in the next five rounds of growth indicate that YKD221 does not assimilate cDCE. Although each culture was diluted to one tenth with fresh W-minimal salt medium on each transfer, the cell concentrations after three days of cultivation were largely similar in the last three rounds of growth. YKD221 might have assimilated carbon dioxide using the acetyl-CoA pathway enzymes for CO_2 fixation; the presence of enzymes of this pathway was suggested by the YKD221 genome sequence. Unexpected growth in the first round appears to be supported by the residual nutrient from the preculture. The 1.9-fold higher cell concentration in the presence of cDCE indicates better growth and more frequent cell division in the presence of cDCE.

When we measured the sizes of cells in the first round of growth following the transfer from LB medium, the average cell size in the presence of cDCE was 2.0 ± 0.5 μm in length by 1.5 ± 0.4 μm in wide, while the average cell size in the absence of cDCE was 1.9 ± 0.4 μm in length by 1.2 ± 0.2 μm in width. The average cell volume in the presence of cDCE was estimated to be 1.7-fold larger than the volume in the absence of cDCE. The higher cell concentration and larger cell volume in the presence of cDCE appeared to result in larger colonies. Although a reason remains to be determined, it is suggested that the presence of cDCE and the residual nutrient from the soil positively affects the first round of growth of YKD221 in minimal salt medium during screening experiments.

Acknowledgments

We thank Dr. Katsumasa Abe for his kind support in IC analysis. This work was supported by a grant from the Ministry of Economy, Trading, and Industry of Japan (Technology development for soil contamination countermeasures).

Supplementary Materials

Supplementary tables are available in our J-STAGE site (http://www.jstage.jst.go.jp/browse/jgam).

References

Arciero, D., Vannelli, T., Logan, M., and Hooper, A. B. (1989) Degradation of trichloroethylene by the ammonia-oxidizing bacterium

Nitrosomonas europaea. *Biochem. Biophys. Res. Commun*., **159**, 640–643.

Arp, D. J., Yeager, C. M., and Hyman, M. R. (2001) Molecular and cellular fundamentals of aerobic cometabolism of trichloroethylene. *Biodegradation*, **12**, 81–103.

Auch, A. F., von Jan, M., Klenk, H. P., and Göker, M. (2010) Digital DNA-DNA hybridization for microbial species delineation by means of genome-to-genome sequence comparison. *Stand. Genomic Sci*., **2**, 117–134.

Ausubel, F. M., Brent, R., Kingston, R. E., Moore, D. D., Seidman, J. G. et al. (1990) Current Protocols in Molecular Biology, 3rd ed., John Willy & Sons, Inc.

Clingenpeel, S. R., Moan, J. L., McGrath, D. M., Hungate, B. A., and Watwood, M. E. (2012) Stable carbon isotope fractionation in chlorinated ethene degradation by bacteria expressing three toluene oxygenases. *Front. Microbiol*., **3**, 63.

Coleman, N. V. and Spain, J. C. (2003) Epoxyalkane: coenzyme M transferase in the ethene and vinyl chloride biodegradation pathways of *Mycobacterium* strain JS60. *J. Bacteriol*., **185**, 5536–5545.

Coleman, N. V., Mattes, T. E., Gossett, J. M., and Spain, J. C. (2002) Biodegradation of *cis*-dichloroethene as the sole carbon source by a beta-proteobacterium. *Appl. Environ. Microbiol*., **68**, 2726–2730.

Futagami, T., Goto, M., and Furukawa, K. (2008) Biochemical and genetic bases of dehalorespiration. *Chem. Rec*., **8**, 1–12.

Goris, J., Konstantinidis, K. T., Klappenbach, J. A., Coenye, T., Vandamme, P. et al. (2007) DNA-DNA hybridization values and their relationship to whole-genome sequence similarities. *Int. J. Syst. Evol. Microbiol*., **57**, 81–91.

Jennings, L. K., Chartrand, M. M., Lacrampe-Couloume, G., Lollar, B. S., Spain, J. C. et al. (2009) Proteomic and transcriptomic analyses reveal genes upregulated by *cis*-dichloroethene in *Polaromonas* sp. strain JS666. *Appl. Environ. Microbiol*., **75**, 3733–3744.

Kageyama, C., Ohta, T., Hiraoka, K., Suzuki, M., Okamoto, T. et al. (2005) Chlorinated aliphatic hydrocarbon-induced degradation of trichloroethylene in *Wautersia numadzuensis* sp. nov. *Arch. Microbiol*., **183**, 56–65.

Leahy, J. G., Byrne, A. M., and Olsen, R. H. (1996) Comparison of factors influencing trichloroethylene degradation by toluene-oxidizing bacteria. *Appl. Environ. Microbiol*., **62**, 825–833.

Li, S. and Wackett, L. P. (1992) Trichloroethylene oxidation by toluene dioxygenase. *Biochem. Biophys. Res. Commun*., **185**, 443–451.

Magnuson, J. K., Stern, R. V., Gossett, J. M., Zinder, S. H., and Burris, D. R. (1998) Reductive dechlorination of tetrachloroethene to ethene by a two-component enzyme pathway. *Appl. Environ. Microbiol*., **64**, 1270–1275.

Mattes, T. E., Coleman, N. V., Spain, J. C., and Gossett, J. M. (2005) Physiological and molecular genetic analyses of vinyl chloride and ethene biodegradation in *Nocardioides* sp. strain JS614. *Arch. Microbiol*., **183**, 95–106.

Mattes, T. E., Alexander, A. K., and Coleman, N. V. (2010) Aerobic biodegradation of the chloroethenes: pathways, enzymes, ecology, and evolution. *FEMS Microbiol. Rev*., **34**, 445–475.

Maymo-Gatell, X., Anguish, T., and Zinder, S. H. (1999) Reductive dechlorination of chlorinated ethenes and 1,2-dichloroethane by "*Dehalococcoides ethenogenes*" 195. *Appl. Environ. Microbiol*., **65**, 3108–3113.

McClay, K., Streger, S. H., and Steffan, R. J. (1995) Induction of toluene oxidation activity in *Pseudomonas mendocina* KR1 and *Pseudomonas* sp. strain ENVPC5 by chlorinated solvents and alkanes. *Appl. Environ. Microbiol*., **61**, 3479–3481.

Murray, R. G. E., Doetsch, R. N., and Robinow, C. F. (1994) Determinative and cytological light microscopy. *In* Methods for General and Molecular Bacteriology, ed. by Gerhardt, P., Murray, R. G. E., Wood, W. A., and Krieg, N. R., pp. 31–32.

Nelson, M. J., Montgomery, S. O., Mahaffey, W. R., and Pritchard, P. H. (1987) Biodegradation of trichloroethylene and involvement of an aromatic biodegradative pathway. *Appl. Environ. Microbiol*., **53**, 949–954.

Newman, L. M. and Wackett, L. P. (1997) Trichloroethylene oxidation by purified toluene 2-monooxygenase: products, kinetics, and turnover-dependent inactivation. *J. Bacteriol*., **179**, 90–96.

Saitou, N. and Nei, M. (1987) The neighbor-joining method: a new method for reconstructing phylogenetic trees. *Mol. Biol. Evol*., **4**, 406–425.

Sambrook, J., Fritsch, E. F., and Maniatis, T. (1989) Molecular Cloning: A Laboratory Manual, 2nd ed., Cold Spring Harbor.

Schäfer, A., Tauch, A., Jäger, W., Kalinowski, J., Thierbach, G. et al. (1994) Small mobilizable multi-purpose cloning vectors derived from the *Escherichia coli* plasmids pK18 and pK19: selection of defined deletions in the chromosome of *Corynebacterium glutamicum*. *Gene*, **145**, 69–73.

Shintani, M., Hosoyama, A., Ohji, S., Tsuchikane, K., Takarada, H. et al. (2013) Complete genome sequence of the carbazole degrader *Pseudomonas resinovorans* strain CA10 (NBRC 106553). *Genome Announc*, **1**, e00488-13.

Simon, R., Preifer, U., and Pühler, A. (1983) A broad host range mobilization system for in vivo genetic engineering: transposon mutagenesis in gram negative bacteria. *Nat. Biotechnol*., **1**, 784–791.

Tamura, K., Peterson, D., Peterson, N., Stecher, G., Nei, M. et al. (2011) MEGA5: molecular evolutionary genetics analysis using maximum likelihood, evolutionary distance, and maximum parsimony methods. *Mol. Biol. Evol*., **28**, 2731–2739.

Tsien, H. C., Brusseau, G. A., Hanson, R. S., and Wackett, L. P. (1989) Biodegradation of trichloroethylene by *Methylosinus trichosporium* OB3b. *Appl. Environ. Microbiol*., **55**, 3155–3161.

Uchiyama, H., Nakajima, T., Yagi, O., and Nakahara, T. (1992) Role of heterotrophic bacteria in complete mineralization of trichloroethylene by *Methylocystis* sp. strain M. *Appl. Environ. Microbiol*., **58**, 3067–3071.

van der Geize, R., Hessels, G. I., van Gerwen, R., van der Meijden, P., and Dijkhuizen, L. (2001) Unmarked gene deletion mutagenesis of *kstD*, encoding 3-ketosteroid Delta1-dehydrogenase, in *Rhodococcus erythropolis* SQ1 using *sacB* as counter-selectable marker. *FEMS Microbiol. Lett*., **205**, 197–202.

Wackett, L. P. and Gibson, D. T. (1988) Degradation of trichloroethylene by toluene dioxygenase in whole-cell studies with *Pseudomonas putida* F1. *Appl. Environ. Microbiol*., **54**, 1703–1708.

Yanisch-Perron, C., Vieira, J., and Messing, J. (1985) Improved M13 phage cloning vectors and host strains: nucleotide sequences of the M13mp18 and pUC19 vectors. *Gene*, **33**, 103–119.